BAND DISCONTINUITY EFFECT ON a-Si:H AND a-SiGe:H SOLAR CELLS

X. XU, A. BANERJEE, J. YANG, AND S. GUHA
United Solar Systems Corp., 1100 West Maple Road, Troy, MI 48084
K. VASANTH, AND S. WAGNER
Department of Electrical Engineering, Princeton University, Princeton, NJ 08544

ABSTRACT

The electrical bandgap of microcrystalline silicon (μc-Si:H) *p* type layers used in a-Si:H alloy solar cells and the band edge discontinuities between μc-Si:H and a-Si:H alloys have been determined by internal photoemission measurements. The bandgap of μc-Si:H is found to be in the range of 1.50 to 1.57 eV, and the discontinuities at the conduction and the valence band edges are 0 to 0.07 and 0.26 to 0.35 eV, respectively. Use of these parameters in the numerical simulation of single-junction a-Si:H and a-SiGe:H alloy solar cells is found to predict experimental results of solar cell performance.

INTRODUCTION

Hydrogenated amorphous silicon (a-Si:H) alloy materials have received a great deal of attention because of their use in low-cost solar cells. Significant progress has been made in the area of multijunction a-Si:H alloy solar cells, and stabilized efficiency of 11.2% and 10.2% have been reported [1,2] for small-area cells and large-area panels, respectively. Microcrystalline (μc) boron-doped layers [3] play a key role in the improvement of the efficiency. As compared to their amorphous counterpart, μc *p*-type layers show lower conductivity activation energy and higher optical transmission, giving rise to higher open-circuit voltage (V_{oc}) and short-circuit current density (J_{sc}) for the solar cell. The properties of the thin *p*-type μc layer used in the cell, however, are not very well understood. Specifically, not much information is available regarding the bandgap of the layer and the band edge discontinuities at the *p*(μc)-intrinsic(*i*) a-Si:H alloy interface. This information is extremely important for reliable numerical simulation of the device performance starting from fundamental material parameters.

Although very little information is available regarding the μc-Si:H/a-Si:H interface, several contradictory reports have been made on the band edge discontinuities between crystalline silicon (c-Si) and the a-Si:H alloys [4-7]. From the measurement of the internal photoemission (IPE) at a c-Si/a-Si:H alloy heterojunction, Mimura and Hatanaka [6] concluded that the major band edge discontinuity occurs in the valence band (ΔE_v = 0.71 eV), while it is only 0.09 eV in the conduction band (ΔE_c). Cuniot and Marfaing [7], on the other hand, used a structure of c-Si/sputtered a-Si:H alloy for IPE measurement and found that the discontinuity in the valence band is negligible, with the main discontinuity existing in the conduction band. We take ΔE_v to be positive when the valence band edge for μc- or c-Si lies above that for a-Si:H or a-SiGe:H in the electron energy diagram (Fig. 1). The opposite is the case for ΔE_c; i.e., ΔE_c is positive when the conduction band edge for μc- or c-Si lies below that for a-Si:H or a-SiGe:H (Fig. 1). In this paper, we present new experimental results of IPE measurements on μc-Si:H/a-Si:H alloy structures and discuss the effect of band edge discontinuities on a-Si:H and a-SiGe:H solar cell performance.

Mat. Res. Soc. Symp. Proc. Vol. 377 © 1995 Materials Research Society

EXPERIMENTAL

The samples for the internal photoemission measurement were deposited on specular stainless steel (ss) substrates without back reflectors. The structure of samples used to measure ΔE_v is ss/*p* μc-Si:H (600 Å)/*i* a-Si:H (100 - 400 Å)/*n* a-Si:H (~100 Å) (#1 and 2 of Table I). The intrinsic a-Si:H layer was grown by rf plasma-enhanced chemical vapor deposition using a disilane-hydrogen mixture. Hydrogen diluted silane was used for μc-Si:H layer deposition. BF_3 and PH_3 were added as dopants for *p* and *n* type doping, respectively. Details of deposition parameters have been reported before [8].

A semitransparent Au or Al front electrode was evaporated on top of the sample to form an Ohmic contact. The monochromatic exciting light of varying wavelength was incident on the front metal electrode. A reverse bias of 50 mV was applied for collecting the photo-generated carriers.

For cell performance studies, a-Si:H and a-SiGe:H alloy solar cells were deposited on ss substrates without back reflectors. The structure of the cells is ss/*n*/*i* a-Si:H (or a-SiGe:H)/*p* μc-Si:H/ITO. The thicknesses of the intrinsic layers are 5000 and 3700 Å for a-Si:H and a-SiGe:H cells, respectively.

Table I. Sample structures for internal photoemission measurement and observed threshold energies.

Sample No.	Structure	E_t (eV)
1	ss/*p* μc-Si:H (600 Å)/*i* a-Si:H (400 Å)/*n* a-Si:H (100 Å)/Au	1.68
2	ss/*p* μc-Si:H (600 Å)/*i* a-Si:H (100 Å)/*n* a-Si:H (100 Å)/Au	1.57
3	ss/*n* a-Si:H (200 Å)/*i* a-Si:H (1000 Å)/*p* μc-Si:H (100 Å)/ITO	1.74
4	ss/*n* μc-Si:H (600 Å)/*i* a-Si:H (100 Å)/*p* μc-Si:H (100 Å)/Al	1.85

DETERMINATION OF ΔE_v AND ΔE_c

According to Kane's model [9] for indirect transitions from semiconductors, the quantum yield Y of internal photoemission in the vicinity of the threshold energy (E_t) can be expressed as

$$Y \sim (h\nu - E_t)^{5/2} \qquad (1)$$

where $h\nu$ is the energy of photons. The internal photoemission process in the ss/*p* μc-Si:H/*i* a-Si:H/*n* a-Si:H/Au sample can be described as follows. The photons that are transmitted through the metal electrode and the thin *n* and *i* layers are partially absorbed in the μc-Si:H layer. The electrons are photoemitted from the valence band of μc-Si:H to the conduction band of a-Si:H (see Fig. 1). The threshold energy, E_{t1}, is the sum of the bandgap, E_g(μc-Si:H), of μc-Si:H, and ΔE_c. Since both *i* and *n* layers are very thin, the predominant contribution to the photocurrent is due to the transition from the valence band of μc-Si:H to the conduction band of the intrinsic a-Si:H alloy.

The 2/5 power of the photoemission quantum yield Y is plotted against the photon energy in Fig.2 for two samples with different thicknesses of the intrinsic a-Si:H layer (#1 and 2 of Table I). As seen in Fig.2, $(Y)^{2/5}$ becomes more linear with $h\nu$ when the *i* a-Si:H layer becomes thinner. For sample #2 with a 100 Å thick *i* layer, a good linear relationship is observed in the range of 1.7 to 2.4 eV. The threshold energy, E_{t1}, is obtained by extrapolating the straight line to the intercept; and 1.57 eV is obtained for sample #2. For the sample with the 400 Å thick *i* a-Si:H layer (sample #1), the contribution of the photogenerated carriers from the *i* layer is not negligible and the intercept energy shifts to around 1.68 eV, which is close to the "threshold energy" of 1.74 eV obtained from 1000 Å thick *i* layer using the configuration of sample #3, i.e., simply the gap energy of a-Si:H.

We performed similar experiments to determine the discontinuity of the conduction band edge between μc-Si:H and a-Si:H layers using the structure #4 of Table I, ss/*n* μc-Si (600 Å)/*i* a-Si (100 Å)/*p* μc-Si (100 Å)/Al. In this case, the threshold energy corresponds to the transition from the top of the valence band of a-Si:H to the bottom of the conduction band of *n* μc-Si:H. This threshold energy, E_{t2}, which is the sum of E_g(μc-Si:H) and ΔE_v, is ~1.85 eV (see Fig. 2).

The discontinuities in both the valence and the conduction band edges between μc-Si:H and a-Si:H can be determined if the value of the mobility gap of a-Si:H is known. Lee et al. measured the mobility gap of a-Si:H using internal photoemission and found that the mobility gap was 0.18 eV wider than the optical gap [10]. If we take this number, the mobility gap of the a-Si:H used in this study should be 1.92 eV (1.74 + 0.18 eV).

Using the values of E_{t1} and E_{t2} obtained from Fig. 2, we can calculate that,

$$\Delta E_v = E_\mu(\text{a-Si:H}) - E_{t1} = 1.92 - 1.57 = 0.35 \text{ eV} \quad (2)$$

$$\Delta E_c = E_\mu(\text{a-Si:H}) - E_{t2} = 1.92 - 1.85 = 0.07 \text{ eV} \quad (3)$$

$$E_g(\text{μc-Si:H}) = E_\mu(\text{a-Si:H}) - \Delta E_c - \Delta E_v = 1.92 - 0.07 - 0.35 = 1.50 \text{ eV}. \quad (4)$$

Based on the determined values of ΔE_v, ΔE_c and the mobility gaps, a schematic band diagram of the μc-Si:H /a-Si:H structure is as shown in Fig.1. It is clear that the discontinuity

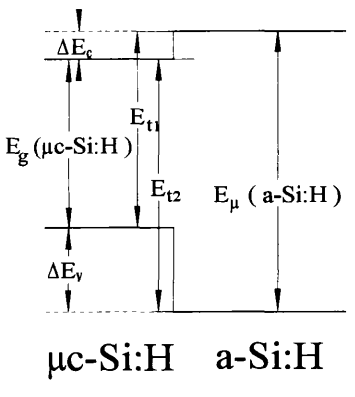

Fig. 1 Schematic band diagram of the μc-Si:H/*i* a-Si:H hetero-structure.

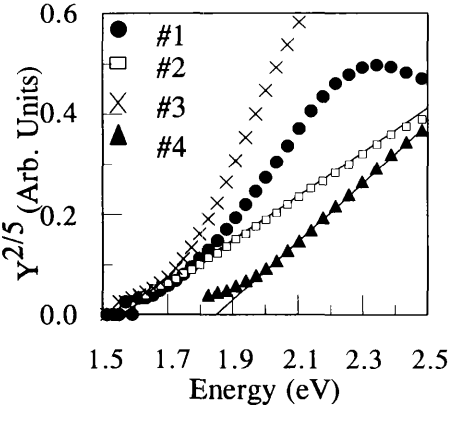

Fig.2 $(Y)^{2/5}$ versus photon energy $h\nu$ for four samples. The lines are eye guide.

occurs mainly in the valence band. Note that the uncertainty in the mobility gap of a-Si:H can result in different values of ΔE_v, ΔE_c and E_g. If the value of the mobility gap of 1.83 eV as recently recommended by Chen and Wronski [11] is used, ΔE_v, ΔE_c and E_g(μc-Si) would be 0.26, 0 and 1.57 eV, respectively. The magnitude of the bandgap between 1.50 to 1.57 eV is consistent with the crystallite size of 80 - 100 Å observed in this material [12].

EFFECT ON a-Si:H CELLS

To study the effect of band edge discontinuities on a-Si:H and a-SiGe:H alloy solar cells with *p* μc-Si:H layers, we have carried out numerical simulations using the AMPS model developed at Penn State University [13]. Calculated a-Si:H cell characteristics are tabulated in Tables II and III, and compared with experimental results. Table II shows that V_{oc} increases (i) as the bandgap of the microcrystalline material increases and (ii) as the discontinuity at the valence band edge decreases. This is understandable since, in both of these cases, the built-in potential increases. We also find very good agreement between theory and experiment (case #3) when the measured values of E_g, ΔE_v, and ΔE_c, as obtained from the IPE measurements, are used in the numerical simulations.

Table II. Simulated and measured a-Si:H alloy cell characteristics. A value of 1.83 eV is used for the mobility gap of a-Si:H in the simulation.

E_g(μc-Si:H) (eV)	ΔE_c/ ΔE_v (meV)	V_{oc} (V)	FF	Case #
1.90	-35/-35	0.99	0.69	1
1.57	260/0	0.98	0.68	2
1.57	0/260	0.93	0.66	3
1.10	60/670	0.53	0.59	4
Measured		0.93	0.65	

Table III. Ratio of Q(-3 V), quantum efficiency under -3 V bias, to Q(0 V), with no bias, for a-Si:H cells as a function of wavelength.

E_g(μc-Si:H) (eV)	ΔE_c/ ΔE_v (meV)	[Q(-3 V)/Q(0 V) - 1]×100 (%) λ (nm) 400	500	600	700	Case #
1.90	-35/-35	1.4	0.9	2.5	5.9	1
1.57	260/0	2.0	1.1	2.5	5.8	2
1.57	0/260	9.9	3.8	3.4	6.7	3
1.10	60/670	65.8	21.2	10.5	14.6	4
Measured		6.6	2.2	2.5	5.8	

Table III shows the effect of bandgap of the *p* μc-Si:H layer and the band edge discontinuities on the ratio of quantum efficiency, i.e. quantum efficiency under -3 V bias to that without bias, Q(-3 V)/Q(0 V), which reflects the loss of carrier collection [14]. In this case also, use of a bandgap of 1.1 eV (that for crystalline silicon) gives a poor fit to the experimental results. The best fit is obtained when the bandgap is taken to be 1.57 eV, and the band discontinuity is assumed to be predominantly in the valence band (case #3). This is consistent with the results from IPE measurement.

EFFECT ON a-SiGe:H CELLS

Simulated and measured values of a-SiGe:H alloy cell characteristics are summarized in Tables IV and V. The optical gap of the a-SiGe:H alloy was measured to be 1.55 eV. In the simulation, a mobility gap of 1.63 eV is used for a-SiGe:H. As in the case of a-Si:H, V_{oc} has a strong dependence on E_g(μc-Si:H) only when E_g is much smaller than the mobility gap of the intrinsic layer. Good agreement between simulated and measured values is obtained for E_g(μc-Si:H) equal to 1.57 eV. This is again consistent with the IPE results. It is interesting to note

Table IV. Simulated and measured a-SiGe:H alloy cell characteristics. A value of 1.63 eV is used for the mobility gap of a-SiGe:H in the simulation.

E_g(μc-Si:H) (eV)	ΔE_c/ ΔE_v (meV)	V_{oc} (V)	FF	Case #
1.90	-170/-100	0.75	0.61	5
1.57	-180/240	0.74	0.57	6
1.57	-90/150	0.74	0.58	7
1.57	0/60	0.74	0.60	8
1.10	-80/610	0.49	0.53	9
Measured		0.74	0.59	

Table V. Ratio of Q(-3 V) to Q(0 V) of a-SiGe:H alloy cells.

E_g(μc-Si:H) (eV)	ΔE_c/ ΔE_v (meV)	λ (nm)	[Q(-3 V)/Q(0 V) - 1]×100 (%) 400	500	600	700	800	Case #
1.90	-170/-100		3.2	0.9	1.0	2.6	2.7	5
1.57	-180/240		1.5	0.6	1.1	3.2	2.6	6
1.57	-90/150		1.3	0.5	0.9	2.7	2.8	7
1.57	0/60		1.4	0.8	1.1	2.8	2.9	8
1.10	-80/610		1.4	0.7	2.1	5.5	5.7	9
Measured			13.4	7.2	5.1	6.9	10.8	

that for a wide range of discontinuity distributions, from zero to maximum offset at either the conduction or the valence band edge, both V_{oc} and FF are remarkably insensitive. This indicates that these parameters are governed more by the bulk properties.

The simulation of quantum efficiency of a-SiGe:H cells is less successful in explaining the experimental results. For all five cases listed in Table IV, the simulated Q ratio, i.e., the loss of carrier collection, is much lower than the measured value (see Table V). Further simulation studies using different bulk and interface parameters will be necessary to understand this discrepancy.

CONCLUSIONS

In conclusion, we have used IPE measurements to determine the electrical bandgap of microcrystalline *p* layers used in a-Si:H alloy solar cells, and the band edge discontinuities at the conduction and valence bands between μc-Si:H and a-Si:H alloy. The bandgap of μc-Si is found to be in the range of 1.50 to 1.57 eV, and the discontinuities at the conduction and the valence band edges are 0 to 0.07 and 0.26 to 0.35 eV, respectively. Use of these parameters in the numerical simulation of single-junction a-Si:H and a-SiGe:H alloy solar cells is found to predict solar cell performance under global AM1.5 illumination. However, further understanding is needed to explain the loss of carrier collection in a-SiGe:H alloy cells.

ACKNOWLEDGMENTS

The authors are grateful to E. Chen, T. Palmer and D. Wolf for experimental assistance. The work at United Solar was supported in part by the National Renewable Energy Laboratory under Subcontract No.ZAN-4-13318-02, and at Princeton by the Amorphous Thin Film Solar Cell Program of the Electric Power Research Institute and the Princeton Plasma Physics Laboratory through a Tuition Fellowship.

REFERENCES:

1. J. Yang and S. Guha, Appl. Phys. Lett. **61**, 2917 (1992).
2. S. Guha, J. Yang, A. Banerjee, T. Glatfelter, K. Hoffman, S. R. Ovshinsky, M. Izu, H. C. Ovshinsky, and X. Deng, Mat. Res. Soc. Symp. Proc. **336**, 645 (1994).
3. S. Guha, J. Yang, P. Nath, and M. Hack, Appl. Phys. Lett. **49**, 218 (1986).
4. F. Evangelisti, J. Non-Cryst. Solids **77&78**, 969 (1985).
5. H. Matsuura and H. Okushi, in Amorphous & Microcrystalline Semiconductor Devices, Vol. II, ed. by J. Kanicki, Artech House (1992), p. 517.
6. H. Mimura and Y. Hatanaka, Appl. Phys. Lett. **50**, 326 (1987).
7. M. Cuniot and Y. Marfaing, Philos. Mag. B **57**, 291 (1988).
8. S. Guha et al., Final Report, SERI/TP-211-3918, National Renewable Energy Laboratory, Golden, Colorado, 1990.
9. E. O. Kane, Phys. Rev. **127**, 131(1962).
10. S. Lee, J. K. Arch, S. J. Fonash, and C. R. Wronski, Proc. 21st IEEE PVSC, 1624(1990).
11. I. Chen and C. R. Wronski, J. Non-Cryst. Solids, to be published.
12. X. Xu, J. Yang, A. Banerjee, S. Guha, K. Vasanth, and S. Wagner, to be published.
13. J. K. Arch, F. A. Rubinelli, J. Y. Hou, and S. J. Fonash, J. Appl. Phys. **69**, 7057 (1991).
14. A. Banerjee, X. Xu, J. Yang, and S. Guha, to be presented in this conference.